Comparative Study of Quantum and Classical Error Correction for Future Quantum-6G Networks

Siddharth Das, Riccardo Bassoli, *Member, IEEE,* Roberto Ferrara, Janis Nötzel, Christian Deppe, Frank H.P. Fitzek, *Senior Member, IEEE,* Holger Boche, *Fellow, IEEE*

***Abstract*—The research on 6G communication networks has started. Currently, the proposed architectures envision the realisation of a fully softwarized network continuum, with in-network intelligence for network management and operations. Moreover, more stringent requirements than 5G have been set in order to support new use cases like telepresence and massive twinning. However, these requirements implies some critical tradeoffs, which are going to limit the promises of 6G. In order to go beyond the intrinsic limitations of 6G, new resources and technologies should be found. That is why, some research groups are now investigating how quantum technologies can be integrated into 6G. This works deals with the scenario of sending classical information via a quantum channel, using the so-called dense coding protocol. If this channel is not ideal, quantum errors can affect the reliability of the communication. Nevertheless, quantum error-correcting codes are still very demanding in terms of resources and redundancy. Then, this work investigates how classical error-correcting codes (in particular, Reed-Solomon codes and turbo codes) can be applied to make reliable classical communications via quantum channels. The preliminary results of this paper show that the employment of classical forward error correction in future hybrid 6G-quantum networks can be very promising.**

***Index Terms*—Dense coding, quantum error correction, error-correcting codes, Reed-Solomon codes.**

I. Introduction

THE standardisation of 5G is reaching its end, and now the research and industrial communities are focusing on the design of future 6G communication networks, which are expected to be deployed from 2030. In Europe, the EU flagship Hexa-X has started defining the architectural and system's aspects of 6G [1]. 6G is expected to host new and very demanding use cases like massive twinning, immersive telepresence for enhanced interactions, Tactile internet and human-machine interaction, robots to cobots, and hyperconnected resilient network infrastructures. In order for the communication system to support these use cases, new Key Performance Indicators (KPIs) were established, which are more demanding than 5G ones [2]. In particular, 6G will demand for the concurrent satisfaction of data rate up to $1\,\mathrm{Tbit\,s^{-1}}$, user-experienced data rate of $1\,\mathrm{Gbit\,s^{-1}}$, end-to-end latency less than 1 ms, frame error rate (reliability) equal to $1 - 10^{-9}$ very high energy efficiency equal to $1\,\mathrm{pJ\,bit^{-1}}$, a connectivity density ten times the one provided by 5G, with an area traffic capacity of up to $1\,\mathrm{Gbit\,s^{-1}\,m^{-2}}$, and density of connected devices greater than $10^6\,\mathrm{km^{-2}}$. Architecturally speaking, the achievement of these KPIs is targeted by designing a specific 6G architecture, which will realise an end-to-end softwarized network continuum to be orchestrated and managed by in-network intelligence. However, the continuous intelligent management of network functions and operations will require huge data mining and processing. With the use of 'classical' communication technologies, the KPIs get stuck into specific trade-offs and inter-dependencies, which are intrinsically limiting the possibilities of 6G to achieve the envisioned goals. That is why, new resources and technologies have been proposed to be integrated in the future 6G networks in order to avoid or to mitigate the correlations among different metrics.

It is expected that, quantum technology will provide resilience by design, device independent security, oblivious transfer and bit commitment [3], making it a worthy extension of 6G. In the first realisation of quantum communication networks, the quantum technologies are expected to be integrated in the existing classical architecture of future 6G networks in order to create a hybrid classical-quantum communication infrastructure [4]. Several large research activities have been started recently to investigate the potential of quantum communication for the application in classical communication networks [5]. In that sense, 6G applications will generate traffic, which will be subsequently encoded into quantum information, to be sent via a quantum channel. This is what happens in dense coding protocol [6], which encodes two classical bits into a flying qubit, allowing for the transmission of classical information with the help of entanglement distribution. It has been shown in [7] that, communication in the presence of entanglement as a resource can enhance the net channel capacity. Nevertheless, the quantum channel is not ideal and various kinds of errors may occur, changing not only the 'value' of a so-called qubit but also modifying its 'phase'. Quantum error correction (QEC) codes have been studied to permit the correction of these errors [4]. The work in [8] were pivotal for understanding QEC schemes — particularly, surface codes. Though in their calculations, to factor a 2000 bit number with an assumed error rate of 10^{-3}, a quantum computer would require 220×10^6 physical qubits; out of which only 10% is used for actual computation while the

S. Das, R. Bassoli and F. H.P. Fitzek are with the Deutsche Telekom Chair of Communication Networks, Institute of Communication Technology, Faculty of Electrical and Computer Engineering, Technische Universität Dresden, Dresden, Germany. R. Bassoli and F. H.P. Fitzek are also with the Centre for Tactile Internet with Human-in-the-Loop (CeTI), Cluster of Excellence, Dresden, Germany. R. Bassoli is also with the Quantum Communication Networks (QCNets) research group, Technische Universität Dresden, Dresden, Germany. (e-mail: {siddharth.das, riccardo.bassoli, frank.fitzek}@tu-dresden.de).

R. Ferrara, J. Nötzel, C. Deppe and H. Boche are with the Department of Electrical and Computer Engineering at Technische Universität München, München, Germany. H. Boche and J. Nötzel are also with the Munich Center for Quantum Science and Technology (MCQST), München, Germany. Holger Boche is also with the Excellence Cluster Cyber Security in the Age of Large-Scale Adversaries (CASA), Ruhr University Bochum, 44801 Bochum, Germany. (e-mail: {roberto.ferrara, janis.noetzel, christian.deppe, boche}@tum.de).

rest is used for QEC. These appalling figures prompts to look for other alternatives in terms of error correction. Energy considerations are another notion that needs to be conscious of while employing a pure QEC, because the storage of qubits in quantum memories with sufficient coherence time is highly energy consuming since the qubits are stored in a super cooled environment [9], [10]. More efficient and effective error-correcting solutions should be researched and proposed to ensure reliability while maintaining energy efficiency.

Classical error correction techniques have been fundamental in the usher of communication technology for several decades. With the legacy of classical error correction, it is logical to pivot in the way of employing classical error correction in combination with a quantum subsystem. In this context, [11] analysed the role of burst errors in a superdense coding setup using classical forward error correction (FEC). Similarly, [12] studied the application of forward error correction for dense coding using several non-binary FEC schemes similar to the current work though there was no direct comparison with any QEC scheme in both of the work.

This paper shows an application of a shortened Reed-Solomon (RS) code with various coding rates and a rate 1/3 Turbo code in a dense coding scenario using MATLAB. The FEC scheme has been pitched against the concatenated QEC code.

II. System Model

A. Superdense Protocol with Classical FEC

The system architecture to simulate the hybrid quantum-classical communication system is depicted in Fig. 1. Here the information is transmitted from one end (Alice) to other (Bob) using superdense coding protocol via a Pauli channel. The forward error correction technique that has been employed is the shortened version of Reed-Solomon (RS) codes [13] and Turbo codes [14]. Selection of a non-binary error correction scheme stemmed from the findings of work done by Boyd et al. [15] who showed that there are certain limitations in terms of capacity while using binary codes and that non-binary codes can have a performance advantage. As it can be seen from Fig. 1 the message bitstream is encoded into RS code before its conversion into quantum symbols. The chosen shortened version of RS code ensures that the code length is even so that there can be a bit-wise pairing of classical information into dense encoded qubit without any extra padding of bits.

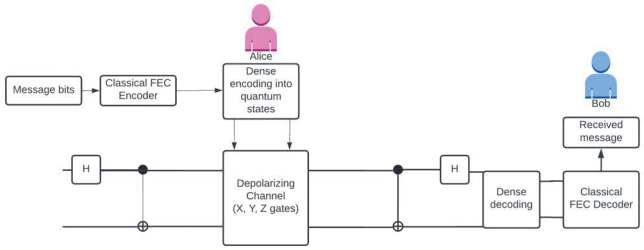

Fig. 1. System model depicting superdense coding protocol combined with Reed-Solomon forward error correction.

The dense coding protocol is instantiated by the entanglement generation between Alice and Bob. The entanglement generation process in the simulator is ideal in nature and does not require any further distillation process. The known Bell-state or *Einstein Podolsky* (EPR) pair that Alice and Bob begins with is

$$\left|\phi^{+}\right\rangle = \frac{1}{\sqrt{2}}(|00\rangle + |11\rangle). \tag{1}$$

Alice uses this state to encode two bits of classical message by the application of unitary operators.

The Pauli error that are being applied on the channel are randomly picked by a random generator. The probability of encountering an error is equally distributed among the Pauli gates X, Y and Z in the simulation and the channel is a *depolarizing channel*. A noisy quantum channel can be described by a completely positive trace preserving (CPTP) linear map λ acting on the quantum state. In the system model described in Figure 1, Alice and Bob share a bi-partite quantum state ρ. Then Alice encodes her qubit locally and sends it to Bob via a noisy quantum channel which is defined as *one-sided* superdense coded channel [16].

An effective modelling of the depolarizing channel which covers several aspects involving the occurrence of errors such as transmission noise, initial state preparation noise and detection/measurement noise can be represented by

$$\lambda_{depolar} = \sum_{i=0}^{3} p_i U_i \rho U_i^{\dagger} \tag{2}$$

where, the probabilities $p_0 \in [0, 1]$ and $p_{i=1,2,3} \in [0, 1/3]$ given that $\sum_i p_i = 1$ and U_i are the Kraus operators which are Pauli matrices [17].

A forward error correction (FEC) scheme, beginning with the case of shortened version of RS (n, k) code has a k-bit input message, possessing a $n{\times}k$ generator matrix that converts the k-bits to n bit codeword. Application of FEC enlarges the intended message by a factor of n/k. In a similar fashion, a parallel-concatenated convolutional code (PCCC) also known as turbo codes (1/3 particularly) takes k input message which is fed into two encoders. First encoder takes the input as it is, while the second encoder takes an *interleaved* message as an input and then outputs a size n codeword. The encoded message — be it in the case of turbo codes or RS codes, is then pair-wise assembled for the dense encoder which encodes each paired classical bits into quantum states by application of suitable gates. If $U(c_0, c_1)$ is an unitary operation on classical bits c_0 and c_1, respectively then $U(c_0, c_1) = X_A^{c_0} Z_A^{c_1}$ denotes the combination of gates that needs to be applied to acquire the possible permutation of two classical bits. Generalising this very notion to the n bit codeword, the ensemble of states that will be ultimately transmitted at Alice's end can be written in the following manner

$$\rho_n = \prod_{i=0}^{n-1} U(c_{2i}, c_{2i+1}) \rho_0 U(c_{2i}, c_{2i+1})^{\dagger}. \tag{3}$$

Here, c_i is the $i-$th bit of the codeword.

At Bob's end, the detection of various quantum states sent my Alice comprises of added errors introduced by the depolarizing channel. All the states are then concatenated back to form a stream of bits so that the RS decoder or the turbo decoder can decode the message. Depending on the distance of chosen code type, the errors can be detected and/or corrected.

The depolarizing limit enforces the scenario where $p_0 = 1-p$ and $p_1 = p_2 = p_3 = p/3$ for $p \in [0, 1]$ from Eq. 2. Which implies, the probability of receiving an incorrect quantum state is $1 - p_0$ but the probability to read an incorrect classical message is slightly less as pointed in [11]. The possibilities that a received Bell-state might have an error are either one, two or no error in the classical bits. This implies for the one-sided dense coding with a depolarizing channel. The frequency a binary message is decoded incorrectly is as following [11] :

$$BER = \frac{2p}{3} \tag{4}$$

where p is the noise parameter.

Therefore, the probability that the original message is received correctly by Bob after the application of FEC under the effect of depolarizing noise is the BER formulated as below:

$$BER = (1-p)^n + \frac{2p}{3}(1-p)^{(n-1)}. \tag{5}$$

B. Superdense Protocol with QEC

The QEC code that has been considered for the comparison is from the class of concatenated codes, specifically — the bit-flip code. Since the quantum simulator had certain limitation to its computational capacity, only simple bit-flip code has been analysed instead of other bigger QEC codes like Shor's 9-qubit [18] code or CSS code or advanced topological codes. A Pauli Z error goes unnoticed in the perspective of a classical bit and because of that, phase-flip or bit-phase-flip QEC schemes have not been included for the comparison.

The entire circuit is depicted in Fig. 2. It can be seen from the bit-flip in the schematic that, the dense protocol is padded with bit-flip correction circuits for each data qubit. An added redundancy of four qubits are required for the application of the bit-flip code. It is to be noted that, the rectangular box E is the only specific location where the occurrence of a bit-flip can be corrected. In other locations it will simply lead to an uncorrectable error in decoding. Fig. 2 describes a concatenated quantum bit-flip correction circuit of coding rate $1/3$.

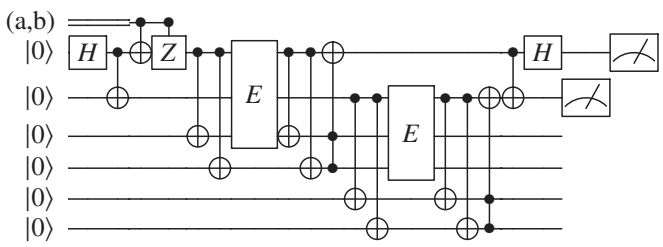

Fig. 2. Superdense protocol with bit-flip QEC.

Similar channel model has been considered for the QEC simulation as it was in sub-section II.A. The first two qubits in the Fig. 2 are the data bits. Subsequent time-steps in the circuit displays the encoding of classical bits (a, b) into qubits by the application of $CNOT$ and $Control-Z$ gates which then passes through the bit-flip correction circuit and then measured by Bob at the other end. The other half of the entangled qubit undergoes through the same procedure.

III. Simulation Platform

The simulator used in the study is a MATLAB based quantum simulator [19]. It is based on David Deutsch's mathematical model of a universal computer. The simulator employs operations such as matrix multiplication and tensor (Kronecker) products to carry out simulations. Both single and multiple qubit gates such as I, X, Y, Z, H, S, T, RX, RY, RZ, U1, U2, U3, CNOT and Toffoli gates are also embedded inside the simulator.

The functioning of the simulator is intuitive. Gates are put into a matrix of *strings*, the row of this matrix represents the number of qubits that have been considered for the computation and column represents the steps of the quantum algorithm. To compute over an arbitrary circuit, the essential steps are 1. formation of quantum algorithm, 2. initialisation of qubits and then 3. passing these values to the quantum computer function which gives the final result of the measurement. A quantum algorithm in the context of the simulator, mimics the actual circuit that is being computed. The algorithm is a matrix composed of strings that represents individual gates. Each column of the algorithm matrix represents the stages of the computation. Once the circuit model has been fed as a matrix, the qubits can be initialised. The function *initializeRegisters* takes in row vectors which represents the qubits as argument. The first argument to the function is considered as the most significant bit (MSB) and the last input is considered as the least significant bit (LSB). After the application of the function initializeRegisters, the function *quantumComputer* is called upon that takes the output of previous two functions — the algorithm and initialised qubits and computes the final result of the entire setup. The final result or the measurement is pushed to the end of the circuit as per the *deferred measurement* principle. This implies that, the simulator will only produce a result if all the stages or time steps of the circuit have been calculated going from left to right. The final output is expressed in computational basis (Z-basis).

To give an example, if one wishes to simply entangle two qubits, the steps to follow as per the simulator is :

1) Initialize the two qubits in the computational basis $|0\rangle$ by calling the function initializeRegisters and passing [1 0] and [1 0] as arguments : init = initializeRegisters([1 0],[1 0]).
2) A quantum algorithm should be formed which is simply the circuit that is being analyzed. In this case an entanglement generation circuit containing Hadamard gate and CNOT gate:

$$algo = \begin{matrix} 'H' & '.' \\ 'I' & 'X' \end{matrix}$$

This forms a matrix of strings representing specific gates.

3) Finally, the variables init and algo is passed inside the function 'quantumComputer' : quantumComputer(algo,[1 2],init), with another parameter which is the number of qubits that are being measured.

After computation, the simulator plots the results in the form of a histogram with probabilities. An example of the above mentioned simulation is depicted below which is an ideal scenario without any errors:

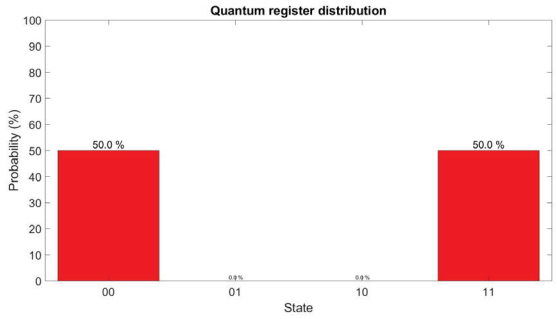

Fig. 3. Simulator result displaying the Bell-state as bar-graphs.

IV. Results and Discussion

The simulation of the presented system model along with the depolarizing noise model has been carried out in MATLAB. In the simulation, the increasing depolarizing probability p were plotted against the classical BER for various coding types summarised in the table I.

Coding	Type	Rate
RS code	(20,10)	0.5
RS code	(20,14)	0.7
RS code	(20,18)	0.9
Turbo code	(3,1)	0.33
QEC	(3,1)	0.33

TABLE I
Types of FEC codes analysed.

Over 5,000 iteration of transmission and reception of frames of size 100 bits have been carried out in dense coding setup to calculate the Bit Error Rate (BER) for each case of RS, Turbo and QEC. The Pauli errors (p_x, p_y, p_z) were applied to the channel by a random generator in MATLAB, thereby acting as a simulated channel. The performance analysis of various FEC codes have been simulated up to a depolarizing noise parameter limit of $p = 0.252$. As observed in the work of [16], going beyond the limit of $p = 0.252$ reaches a channel capacity comparable to that of a classical channel and the sender does not benefit from the dense coding protocol anymore.

A. RS Code vs Bit-flip repetition Code

The comparative analysis of RS code and the quantum bit-flip code has been plotted in Fig. 4.

For the RS code cases, the coding rate has been gradually increased to see how the decoding capability functions in the presence of higher depolarizing noise probability. The RS $(20, 10)$ has a code rate of 0.5 with a correction capability up

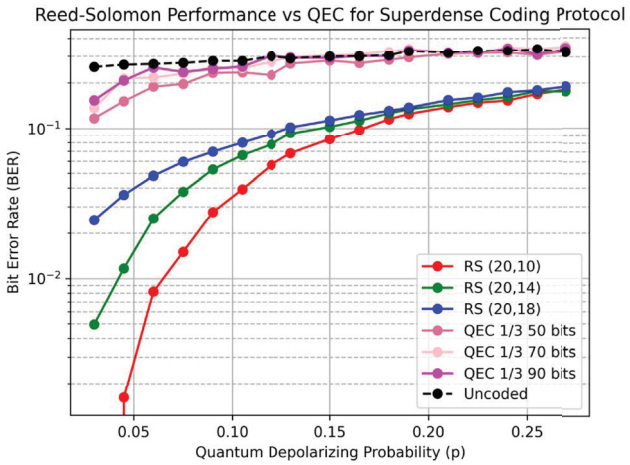

Fig. 4. BER versus quantum depolarizing probability p for the classical FEC - RS code and Quantum bit-flip code.

to 5 symbols. Each symbol throughout the entire simulation contains 5 bits making a total of 100 bits. Due to a larger hamming distance, RS code $(20, 10)$ outperformed its counterparts at the cost of lower channel capacity. The coding rates were then increased from 0.5 to 0.7 and 0.9 for the case of RS $(20, 14)$ and $(20, 18)$ respectively. The increase in code rate has deteriorated the performance of the RS code types $(20, 14)$ and $(20, 18)$. At $p = 0.03$ there is a net difference of 10^{-2} in BER between RS $(20, 10)$ and RS$(20, 18)$. At a value of depolarizing probability of $p = 0.15$ it can be observed from the Fig.5 that the difference among various coding types is quite less and all of them have a cross-over point beyond $p = 20$. The complete randomization of a qubit imposed by the depolarizing channel at high depolarizing noise beyond $p = 20$ leads to an increase of error that is more than the correction capability of the RS codes and hence the BER performance keeps degrading with increasing depolarizing noise.

In the QEC-bit-flip code, the code rate was kept constant due to the limitation of the simulator. The simple bit-flip code has been employed for Alice's and Bob's qubits. From the Fig.4, it is evident that RS codes transcend over the QEC-bit-flip code in terms of performance. There is a difference of 2 orders between the RS $(20, 10)$ and the QEC- bit-flip code. It is interesting to note that, the QEC scheme is quite close to the uncoded information bits in terms of BER performance. It clearly signifies the fragility of qubits even after a QEC scheme.

B. Turbo Code vs Bit-flip repetition Code

Apart from RS code, this paper extends its analysis to the Shannon capacity-reaching error correction technique of Turbo codes. The MATLAB turbo decoder is based on parallel concatenated convolutional decoding scheme which uses the soft-in-soft-out (SISO) a posterior probability [20].

A frame of 128 bits were sent and received via the depolarizing channel for a round of 5000 to refine the BER

ISBN 978-3-8007-6001-5

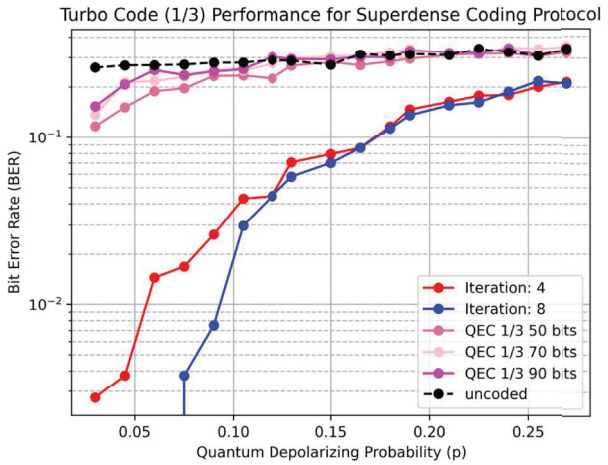

Fig. 5. BER versus quantum depolarizing probability p for the classical FEC - Turbo code and Quantum bit-flip code.

values and the depicted plot in Fig. 5 was generated. As it can be seen from the Fig. 5, eight iterations of the turbo code displays a reasonable performance though, outperforming QEC code. The dense decoder at Bob's end, as displayed in Fig. 1 is a hard decoder, i.e. the dense decoder outputs a hard decision. Since the turbo decoder uses a SISO based approach, it is more likely for turbo codes to have an enhanced performance in a modulated additive white gaussian noise (AWGN) channel where the decisions are soft and the decoders exchange iteratively the soft input from the demodulator and converge towards the right solution. Increasing the number of iterations at the decoder side is another overhead which raises the complexity. Nevertheless, the turbo codes displayed better tolerability in the presence of error than the QEC scheme.

The performance of turbo code can be readily increased from a code rate of $1/3$ to $1/2$ by employing puncturing.

V. Conclusion

The article has analysed the application of RS codes and Turbo codes for reliable communications via an erroneous quantum channel in dense coding scenario. The results have shown significant potentials of classical error correction in providing reliability in classical communications over quantum channels. Comparison between classical FEC and QEC strongly favoured the classical means of error correction. Retrofitting the current work with combination of symbol-based encoder/decoder can lead to more efficient coding paradigms that can nearly reach Shannon's channel capacity [21]. The idea of treating the quantum encoder and decoder in a dense coding setup as a SISO based system can greatly enhance the performance of the classical FEC. The realisation of current work opens up avenues for future quantum network models [22], [23] as the classical FEC can be used at the link layer of the quantum protocol stack to correct errors encountered in the physical layer. For the near-term future a classical-quantum stack model will be an eventuality where the quantum notion will be embedded inside the already present classical layer; for such a system the deployment of classical FEC can have a seamless integration in such a complex hybrid network. Thereby, avoiding dependence on higher dimensional quantum based error correction schemes which are known to be fragile and resource demanding.

Acknowledgment

This work has been partially funded by the German Research Foundation (DFG, Deutsche Forschungsgemeinschaft) as part of Germany's Excellence Strategy – EXC2050/1 – Project ID 390696704 – Cluster of Excellence "Centre for Tactile Internet with Human-in-the-Loop" (CeTI) of Technische Universität Dresden. The authors also acknowledge the financial support by the Federal Ministry of Education and Research of Germany in the programme of "Souverän. Digital. Vernetzt.". Joint project 6G-life, project identification number: 16KISK001K and 16KISK002. Janis Nötzel received funding via DFG grant:NO 1129/2-1. Holger Boche also thanks the DFG within Germany's Excellence Strategy EXC-2111—390814868 and EXC-2092 CASA-390781972 for the support.

References

[1] Hexa-X. (2022, Feb.) Deliverable D1.3 Targets and requirements for 6G - initial E2E architecture.

[2] R. Bassoli, F. H. Fitzek, and E. Calvanese Strinati, "Why do we need 6G?" *ITU Journal on Future and Evolving Technologies*, vol. 2, no. 6, pp. 1–31, 9 2021.

[3] G. P. Fettweis and H. Boche, "6g: The personal tactile internet—and open questions for information theory," *IEEE BITS the Information Theory Magazine*, vol. 1, no. 1, pp. 71–82, 2021.

[4] R. Bassoli, H. Boche, C. Deppe, R. Ferrara, F. H. P. Fitzek, G. Janßen, and S. Saeedinaeen, *Quantum Communication Networks*, 1st ed. Springer International Publishing, Jan. 2021.

[5] F. Fitzek and H. Boche, "Research landscape – 6g networks research in europe: 6g-life: Digital transformation and sovereignty of future communication networks," *IEEE Network*, vol. 35, no. 6, pp. 4–5, Nov 2021.

[6] C. H. Bennett and S. J. Wiesner, "Communication via one- and two-particle operators on einstein-podolsky-rosen states," *Phys. Rev. Lett.*, vol. 69, pp. 2881–2884, 1992. [Online]. Available: https://link.aps.org/doi/10.1103/PhysRevLett.69.2881

[7] J. Nötzel and S. DiAdamo, "Entanglement-assisted data transmission as an enabling technology: A link-layer perspective," in *2020 IEEE International Symposium on Information Theory (ISIT)*, 2020, pp. 1955–1960.

[8] A. G. Fowler, M. Mariantoni, J. M. Martinis, and A. N. Cleland, "Surface codes: Towards practical large-scale quantum computation," *Physical Review A*, vol. 86, no. 3, Sep 2012. [Online]. Available: http://dx.doi.org/10.1103/PhysRevA.86.032324

[9] Y.-W. Cho, G. T. Campbell, J. L. Everett, J. Bernu, D. B. Higginbottom, M. T. Cao, J. Geng, N. P. Robins, P. K. Lam, and B. C. Buchler, "Highly efficient and long-lived optical quantum memory with cold atoms," in *2017 Conference on Lasers and Electro-Optics (CLEO)*, 2017, pp. 1–2.

[10] E. Saglamyurek, N. Sinclair, J. Jin, J. S. Slater, D. Oblak, F. Bussieres, M. George, R. Ricken, W. Sohler, and W. Tittel, "Quantum memory for quantum repeaters," in *2011 International Quantum Electronics Conference (IQEC) and Conference on Lasers and Electro-Optics (CLEO) Pacific Rim incorporating the Australasian Conference on Optics, Lasers and Spectroscopy and the Australian Conference on Optical Fibre Technology*, 2011, pp. 420–420.

[11] R. J. Sadlier and T. S. Humble, "Superdense coding interleaved with forward error correction," *Quantum Measurements and Quantum Metrology*, vol. 3, no. 1, 2016.

[12] C. E. Boyd, "Classical error-correcting codes in quantum communications," 2014.

[13] I. S. Reed and G. Solomon, "Polynomial codes over certain finite fields," *Journal of the society for industrial and applied mathematics*, vol. 8, no. 2, pp. 300–304, 1960.
[14] C. Berrou, A. Glavieux, and P. Thitimajshima, "Near shannon limit error-correcting coding and decoding: Turbo-codes. 1," in *Proceedings of ICC '93 - IEEE International Conference on Communications*, vol. 2, 1993, pp. 1064–1070 vol.2.
[15] C. Boyd, R.-A. Pitaval, Parts, and O. Tirkkonen, "Non-binary classical error-correcting codes for quantum communication," in *2015 IEEE International Conference on Communications (ICC)*, 2015, pp. 4060–4065.
[16] Z. Shadman, H. Kampermann, D. Bruß, and C. Macchiavello, "Optimal superdense coding over memory channels," *Physical Review A*, vol. 84, no. 4, p. 042309, 2011.
[17] M. A. Nielsen and I. Chuang, "Quantum computation and quantum information," 2002.
[18] P. W. Shor, "Scheme for reducing decoherence in quantum computer memory," *Phys. Rev. A*, vol. 52, pp. R2493–R2496, Oct 1995.
[19] M. V., "Quantum computer simulator," 2021. [Online]. Available: https://www.mathworks.com/matlabcentral/fileexchange/73035-quantum-computer-simulator
[20] S. Benedetto, D. Divsalar, G. Montorsi, and F. Pollara, "A soft-input soft-output maximum a posteriori (map) module to decode parallel and serial concatenated codes," *TDA progress report*, vol. 42, no. 127, pp. 1–20, 1996.
[21] Z. Babar, S. X. Ng, and L. Hanzo, "Near-capacity code design for entanglement-assisted classical communication over quantum depolarizing channels," *IEEE Transactions on Communications*, vol. 61, no. 12, pp. 4801–4807, 2013.
[22] A. Pirker and W. Dür, "A quantum network stack and protocols for reliable entanglement-based networks," *New Journal of Physics*, vol. 21, no. 3, p. 033003, 2019.
[23] W. Kozlowski, A. Dahlberg, and S. Wehner, "Designing a quantum network protocol," in *Proceedings of the 16th International Conference on emerging Networking EXperiments and Technologies*, 2020, pp. 1–16.